Written Report on the analysis and comparison of Ground-based and Space-based image data using a simplified differential photometry workflow.

<u>Prepared as part of undergraduate coursework</u>

(Astronomical Techniques, University of Southern Queensland)

Warren Van Ryn,

15 May 2023

PHY2204 – Astronomical Techniques, University of Southern Queensland, Toowoomba, Queensland, Australia

This report is presented in its assessed form with minor editorial revisions for clarity. No reprocessing of the original observational data has been performed.

1.0 Introduction/Abstract

This project investigated and documented the process of analysing ground-based and space-based pre-prepared image data, using AstroImageJ(Collins et al. 2017) software (available via download from the University of Louisville) where applicable, to reduce the data and perform differential photometry on each data-set. The supplied ground-based digital images used for this report were taken at Mt Kent Observatory, Toowoomba, Queensland between 12.29:15 and 16:01:24 UTC on 07/08/2018 and will be used to view/confirm a transiting exoplanet orbiting WASP-44(Strasbourg/CNRS 2023a). The image files used to identify a transiting exoplanet using space-based observations is from TESS(National Aeronautics and Space Administration 2022) and is comprised of images taken between UTC18:24:05.560 on 11/12/2021 and 02:45:05.391 on 16/12/2021, these will be used to view/confirm an exoplanetary transit of KELT-17(Strasbourg/CNRS 2023b). The processes and methods used to undertake this investigation will be outlined and the results will be presented, analysed and discussed. A basic mathematical analysis will be performed on each data-set's results and compared to known/accepted values, with any discrepancies and error analysis discussed. A brief comparison of the methods, analytical processes and results involved in ground-based and space-based photometry image analysis will be presented based on the results of this investigation.

1.1 Background Information

One of the more successful modern techniques for locating and studying the physical characteristics of exoplanets utilises the approach of observing transiting planets in the combined light of the planet–star system. The techniques and disciplines of exoplanet transit photometry and spectroscopy currently yield a large amount of data advancing our comprehension of exoplanetary properties and atmospheres. Current contrast-style transit studies range from brightness contrasts of one part per hundred to greater than one part per 10,000 and are obtainable with existing ground and space-based telescopes.(Seager 2008)

There is a distinction to be made between Photometry and Radiometry in relation to the wavelengths being observed but as the example image sequences used in this investigation are within the visible spectrum, the term photometry will be used for convenience and clarity.

Photometry in astronomy is the measurement of electromagnetic energy coming to us from an astronomical object within a selected range of wavelengths(Kitchin 2020, p. 287). Specifically, photometry is a method used in astronomy that is focused on measuring the flux or intensity of light radiated by astronomical objects. This light is measured through a telescope attached to a photometer, which is often constructed using electronic devices such as CCD photometers or photoelectric photometers that converts light into an electric current via the photoelectric effect. When calibrated correctly against comparison stars (or other light sources) of known intensity and spectral parameters, photometers can measure the brightness or apparent magnitude of celestial objects to a high degree of precision.

The variety of methods used to perform photometry depend on the wavelength region under study. However, at its most fundamental level, photometry is conducted by collecting light and passing it through specialised photometric optical bandpass filters, then capturing and recording the light's energy with a photosensitive device. Numerous standard arrangements of passbands (called photometric systems) are defined to facilitate accurate comparison of observations.

Various types of photometry are often used in the observation/detection of transiting exoplanets. The one used in this report applies the methods of *differential photometry*, that simultaneously measure the brightness of a target object and select nearby similar stars in the image simultaneously. Rather than measure the magnitude of a star on an absolute scale, measurements are made over time relative to one or more non-variable star(s) and these differences are then plotted to study and illustrate the relative or differential change in magnitude. In this manner, the minute decreases in magnitude of a star hosting an exoplanet are studied and properties of the orbiting planet can be determined.

Differential photometry is less complicated than some of the other photometry techniques and is useful for time series observations. When undertaking CCD photometry, both the target and comparison objects are

observed at the same time, with the same filters, using the same instrument, and viewed through the same optical path. Most of the observational variability drops out and the differential magnitude is simply the difference between the instrument magnitude of the target object and the comparison object(s). This is very useful when plotting the change in magnitude over time of a target object.

A plot of magnitude against time produces a light curve, yielding considerable information about the physical process causing the brightness changes. One fundamental physical parameter that can be derived from the photometry of a transiting planet is radius. A normal star is at roughly constant brightness, till an exoplanet transits the star. During the exoplanet transit, the starlight drops in the ratio of the planet-to-star area; if the radius of the star is known the exoplanet radius can be determined(Seager 2008).

A vital part of applied *differential photometry* lies in the selection of the comparison stars. This/these should be non-variable, close to the star of interest, of similar apparent magnitude and spectral class and have its/their own magnitudes sufficiently known reliably on the photometric system that is in use. Amongst the brightest stars there is usually some difficulty in finding a suitable comparison star that is close enough. With fainter stars, the likelihood that a suitable companion star exists is higher, but the chance of its details being known are less. Thus finding perfect comparison stars to use for this method of analysis can potentially be problematic or less than ideal(Kitchin 2020, p. 305).

The Software used in this investigation to process/reduce the supplied image data-sets and produce differential photometry light curve plots is **AstroImageJ**(AIJ), which provides an astronomy specific image display environment and tools for astronomy specific image calibration and data reduction. AIJ is streamlined for time-series differential photometry, light curve detrending and fitting, and light curve plotting, especially for applications requiring ultra-precise light curves (e.g., exoplanet transits). AIJ reads and writes standard Flexible Image Transport System (FITS) files, provides FITS header viewing and editing, and is World Coordinate System aware, including an automated interface to the astrometry.net web portal for plate solving images. AIJ provides research grade image calibration and analysis tools with a GUI driven approach.(Collins et al. 2017). Further information regarding the software can be found at https://www.astro.louisville.edu/software/astroimagej/index.html

Calibration of the images is done to improve the signal to noise ratio as much as possible and account for environmental and equipment effects on the final image. Dark, flat and bias frames are used to adjust the *light* frames of the raw images captured. The noise in a CCD image is dependent primarily on the temperature of the telescope/camera. A dark frame taken at the same temperature as an image, therefore, will have approximately the same noise, making it possible to subtract this noise from the image. However, there are still slight variations in the amount of noise from dark frame to dark frame. Flats are used to remove image artifacts caused by the optical system. Vignetting and shadows from unfocused dust specks are a common aberration which flats remove. A flat is simply a blank, evenly illuminated image which will show the variations in brightness due to the optical system. By subtracting this image from the uncalibrated celestial image, the effect of these aberrations is vastly reduced. Bias is the term used to describe a CCD camera's pixel-to-pixel variation at zero. Each pixel has a slightly different base value, and this bias is removed using a bias frame. Since dark frames contain the same bias as a light frame, dark-subtracted images are already bias-subtracted. But some new cameras do not require dark frames, as they have very low dark current, so a bias frame could be used for images taken with such a setup. Also, a bias frame can be used to scale a dark frame if a dark frame is not equal in exposure time to the light frame from which it will be subtracted. AstroImageJ will be used to produce master files of these frame types for calibration purposes. Whilst preparing these frame types and applying them to our image data-set, median values will be used rather than the average. This approach is used for this investigation as a median value provides a less skewed result if outliers exist, which is expected/anticipated in this case and should be prepared for when reducing and preparing our initial data-sets. Phenomena such as cosmic rays can cause extreme flux/charge values and therefore produce spikes in the image data-set that need to be removed. Average value sampling during the data calibration process would not remove these outlier values.

Multiple-aperture Stacking and aligning of the individual images within the data-set so as to produce a time plotted light curve for analysis will also be undertaken using AstroImageJ. Care will be taken to choose aperture values appropriate to the qualities of the data-set along with qualities appropriate to the star under investigation. Central aperture size settings will be set large enough to capture/encompass the target and chosen comparison stars. An aperture setting too small will miss capturing the full extent of the star's visible

radiated flux, whilst with apertures set too large additional pixels are present that do not add any information/signal to the process. Care will also be taken with the aperture(s) outer-ring background flux calculation area. Care will be taken to ensure this part of our aperture settings is large enough to get a good statistical sample of the background of the image surrounding the Star selected via multi-aperture process prior to stacking the raw data-set. This outer portion of the aperture will be subtracted from photometric calculations produced by AstroImageJ regarding the chosen target and comparison stars.

The two target stars being examined for plotted light-curve evidence of a transiting exoplanet are WASP-44 and KELT-17.

WASP-44 is a G-type star, slightly less massive and slightly smaller than the sun. It is also slightly cooler but more metal rich than our sun. WASP-44 was identified as an exoplanet candidate in 2009 by the Superwasp project and confirmed via doppler spectroscopy in 2011(Anderson et al. 2012). For the purposes performing analysis on the light-curve plotted in AstroImageJ the following values will be used for WASP-44:

Spectral Type: G-type (GV8)
Mass: 0.917 M_{sun} (Mancini et al. 2013) = 1.99×10^{30}kg X 0.917
Radius: 0.963912 R_{sun} = 0.963912 X 6.99508×10^{8}m (The California Institute of Technology 2023a)
Distance: 364.512pc (The California Institute of Technology 2023a)
Apparent Magnitude(V): 12.9
Temperature: 5410 K
Metallicity: 0.006

KELT-17 is more massive than our sun and was confirmed to have an exoplanet in 2016(Zhou et al. 2016).This host star was only the fourth A-type star with a confirmed transiting planet, and it is one of the most massive and rapidly rotating planet hosts. It has a solar or slightly sub-solar levels of metallicity(Saffe et al. 2020).For the purposes performing analysis on the light-curve plotted in AstroImageJ the following values will be used for KELT-17:

Spectral Type: A-type
Mass: 1.732 M_{sun} = 1.99×10^{30}kg X 1.732
Radius: 1.70169 R_{sun} = 1.70169 X 6.99508×10^{8}m
Distance: 226.5pc
Apparent Magnitude(V): 9.29
Absolute Magnitude: 2.68
Temperature: 7511 K
Metallicity: -0.0180
(The California Institute of Technology 2023b)
(exoplanet kyoto organisation 2023)

The comparison stars chosen to complement the photometric analysis of these two stars will be chosen of similar size, type and brightness where possible. Care will also be taken to choose comparison stars that are not variable in nature so as not to affect the differential nature of the analysis.

1.2 Theory

The relevant equations and mathematical calculations used for producing the photometry light curve plot will be performed by the software. The basic mathematical formula that will be used to perform simple planetary radius calculations is shown below.

$$R_p = R_{star}\sqrt{dip} \qquad \text{(Eqn 1)}$$

Where:
R_p is the radius of the transiting planet.
R_{star} is the radius of the host star.
dip is the change in magnitude calculated from the time-based light-curve plot.

There are many other properties of the star and the planet that can be derived from this form of analysis, but these are beyond the scope of this investigation and its associated report.

2.0 Methodology

2.1 Equipment List

Desktop or laptop computer with an online connection.
AstroImageJ software. (https://www.astro.louisville.edu/software/astroimagej/index.html)
WASP-44 data-set.
KELT-17 data-set.

2.2 Procedure

Pre-existing workflow knowledge of astrophotography software, calibration and stacking processes allowed reasonable comprehension of the AstroImageJ user-manual during this procedure. The standard workflows and process values outlined via the AstroImageJ user-manual were followed.

- ECMA(javascript) libraries and runtimes updated to current versions.
- Downloaded and installed AstroimageJ software from https://www.astro.louisville.edu/software/astroimagej/installation_packages/
- The RAW image sequence for WASP-44 was imported into AstroImageJ. Care was taken to confirm the correct number of files were imported and the virtual stack option was enabled due to the number of files.
- Opened CCD data processing window, set working directories and save options. Processed the provided Darks and Flats files into a MasterDark and MasterFlat file (no bias image frames were provided within this data-set). Care was taken during this step to ensure median rather than average calculations were used for the reasons outlined in the background section of this report (cosmic ray strikes on the detector primarily).
- Opened/imported calibration processed image sequence and set aperture value settings to values appropriate (12-18-30) to use for stack alignment purposes on this image-set. Values chosen encompassed target and similar size target stars and provided enough BG detail to deduct from calculations performed on this image set.
- Selected ‘align stack using apertures’ function, confirmed correct options selected (no advanced options mostly). Selected target and comparison stars for alignment process and initiated stack alignment.
- Opened/imported calibrated_aligned processed image sequence and opened CCD data processing window.
- Selected working calibrated_aligned image sequence directory within DP window, setup process sub-directory and suffix info.
- General (not plate solved) FITS header update process initiated to ensure correct HJD info included within data-set headers, with manual entry info for WASP-44 determined using the pop-up ‘DP coordinate info converter’ window. WASP-44 used as SIMBAD object ID and Mt. Kent was used as the observatory location. Correct target star determined using SIMBAD image.c
- Opened/imported calibrated_aligned_fitsupdated image sequence and reopened CCD data processing window. Initiated Photometry post processing functions with multi-aperture and plot settings enabled
- Aperture setting set to 12-18-30, as determined earlier to be optimal on this image sequence, and centroid apertures option enabled in ‘multi-aperture measurements’ popup window. Place apertures option/button selected.

- Selected WASP-44 as target star (using SIMBAD images as visual reference to determine correct target star). Allowed AstroImageJ to suggest/auto-select 5 comparison stars and manually added an additional 5 comparison stars prior to confirming photometry post processing. Viewed and saved outputs of produced light curve and associated plot information. Noted values at end of time sequence and decided against additional outlier removal as being necessary for accurate analysis.
- A truncated procedure was used for the KELT-17 data-set. Calibration, alignment and FITS header updates were not necessary on the KELT-17/TESS data-set. Post processing was initiated directly on the data-set.
- Aperture settings for the TESS images were set to (smaller) values of 5-12-20 as resolution, star size and signal to noise ratio of background very different to Mt Kent data-set. Centroid apertures enabled in 'multi-aperture measurement' popup window. Place apertures option/button selected.
- Selected KELT-17 as target star (using SIMBAD images as visual reference to determine correct target star). Allowed AstroImageJ to suggest/auto-select 4 comparison stars and manually added an additional 3 comparison stars prior to confirming photometry post processing (manual additions used to increase odds of non-appropriate comparisons for educational purposes). Viewed and saved outputs of light-curve plots. Noted interesting dip in one of the selected comparison stars.

3.0 Results and Analysis

3.1 Mount Kent Results & Analysis

The image shown below shows WASP-44 (T1) target star along with the chosen comparison stars used during photometry post processing in AstroImageJ.

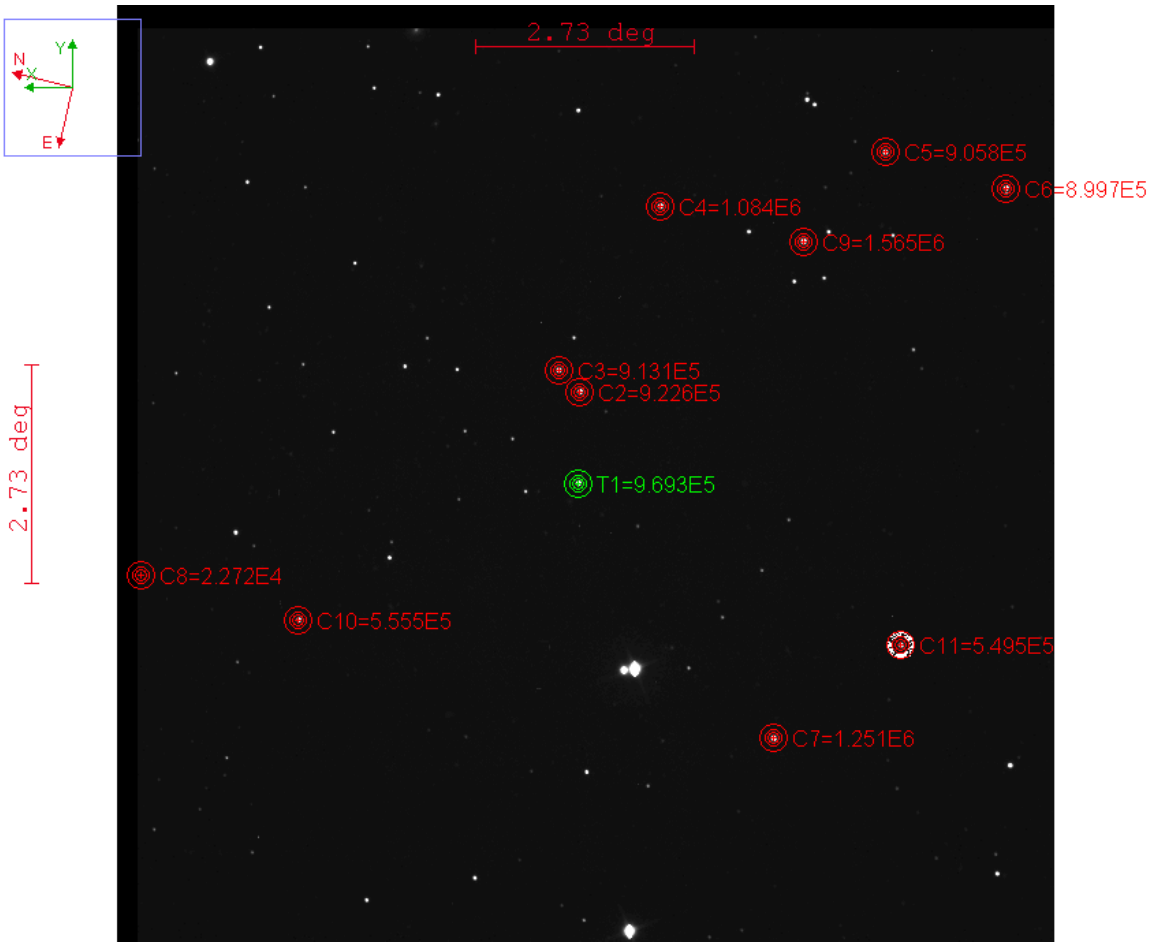

Figure 1: AstroImageJ field view of the WASP-44 target star (T1, green aperture) and selected comparison stars (C1–C10, red apertures) used for differential photometry of the Mt Kent Observatory data set. Aperture placement and sizing were chosen to encompass the stellar PSF while allowing background estimation via outer annuli.

The image displayed below in fig.2 shows the initial photometry light-curve plot for WASP-44, which includes all comparison stars.

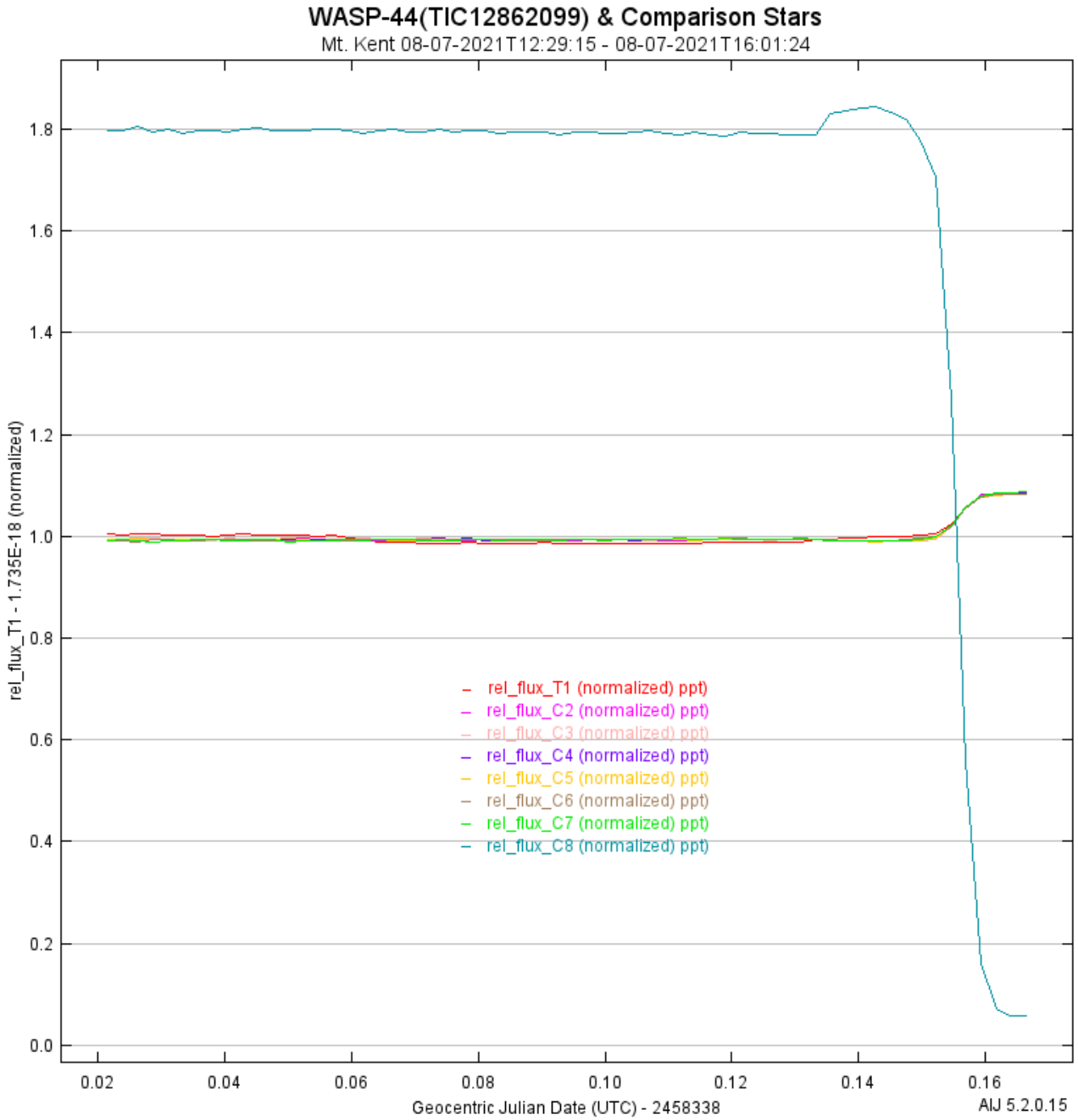

Figure 2: Initial differential photometry light curve for WASP-44 showing the target star and all selected comparison stars prior to quality filtering. The x-axis represents heliocentric Julian date (HJD) and the y-axis shows normalised relative flux. Several comparison stars exhibit variability unsuitable for precise differential analysis.

The plot shown in fig.3 below shows target and comparison stars with comparison stars showing properties unsuitable for differential analysis removed from the plot to allow cleaner data. Data-points towards the end of the data will be discarded when making manual calculations. Comparison star C8 was removed from the plotted data. The plot was shifted to display the usable portion of the data-set.

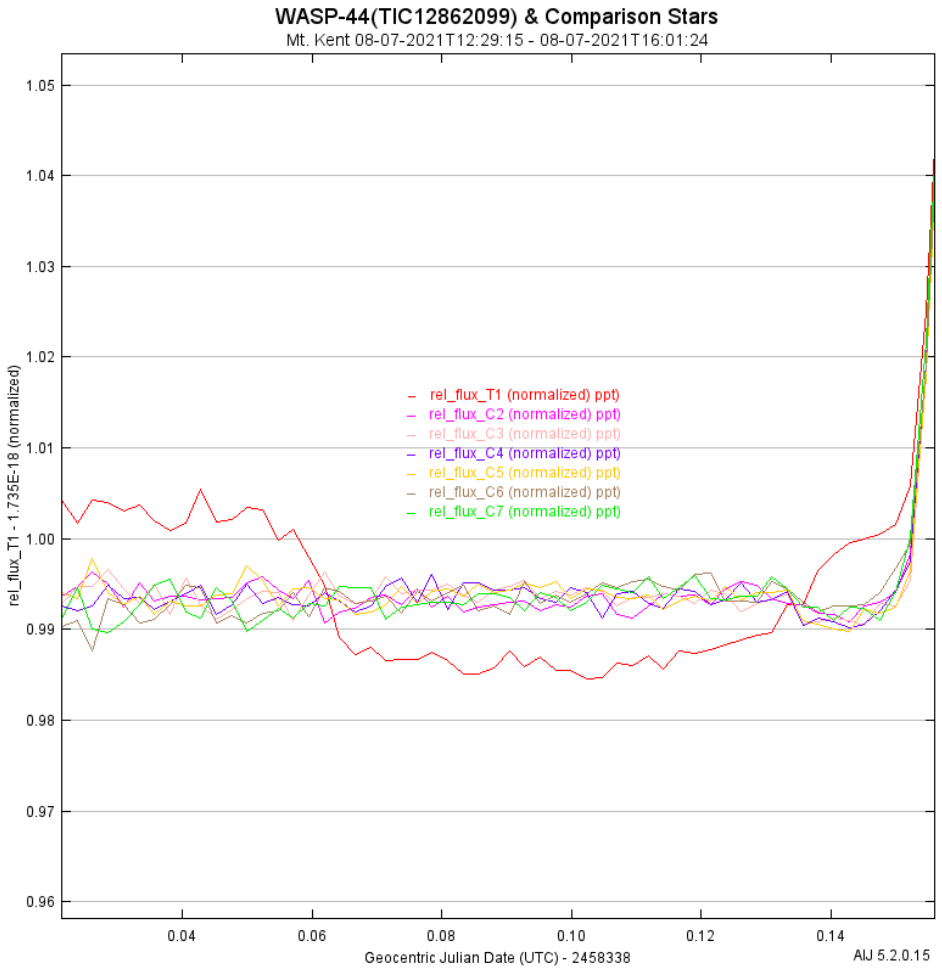

Figure 3: Differential photometry light curve for WASP-44 after removal of variable comparison stars (C8 excluded). The remaining comparison stars show stable behaviour over time, allowing the transit-related flux decrease of the target star to be more clearly identified. The plotted time range has been truncated to exclude unusable end-of-sequence data.

Plotted output was saved in table format and values for individual data-points used to calculate the change in flux values. Baseline averages were calculated only from data taken from the pre-dip portion of the data-set of WASP-44's light-curve. Average values for the dips were calculated by taking an average of all values within the dip. The results of Dip calculation performed in excel are shown below along with subsequent planetary radius calculations.

Average value of pre-dip measurements = 0.103619775

This will be used as a baseline to calculate the dip (change in flux) value.

dip average value = 0.102311482 (using excel)

$DIP = 1 - dip_{av}/baseline_{av} = \Delta$ flux = 0.0126259008

From Eqn1:

$R_p = R_{star}\sqrt{DIP} = 0.963912R_{sun}\sqrt{0.0126259008}$
$= (0.963912 \times 6.95508 \times 10^8)\ \sqrt{0.0126259008}$
$= 75330474.52m = 75330.47452km$
$= 1.077519625\ R_{jup} = 11.82396398\ R_{earth}$

The known/accepted value chosen from the Exofop - TESS(The California Institute of Technology 2023a) resource provides a planetary radius value of 12.3299 R_{earth}.

The percentage error difference for the results calculated are shown below:

(75330474.52m – 78553792.9m / 78553792.9) x 100% = -4.103326219% = -4.1%

3.2 TESS Results & Analysis

The image shown below shows KELT-17 (T1) target star along with the chosen comparison stars used during photometry post processing in AstroImageJ.

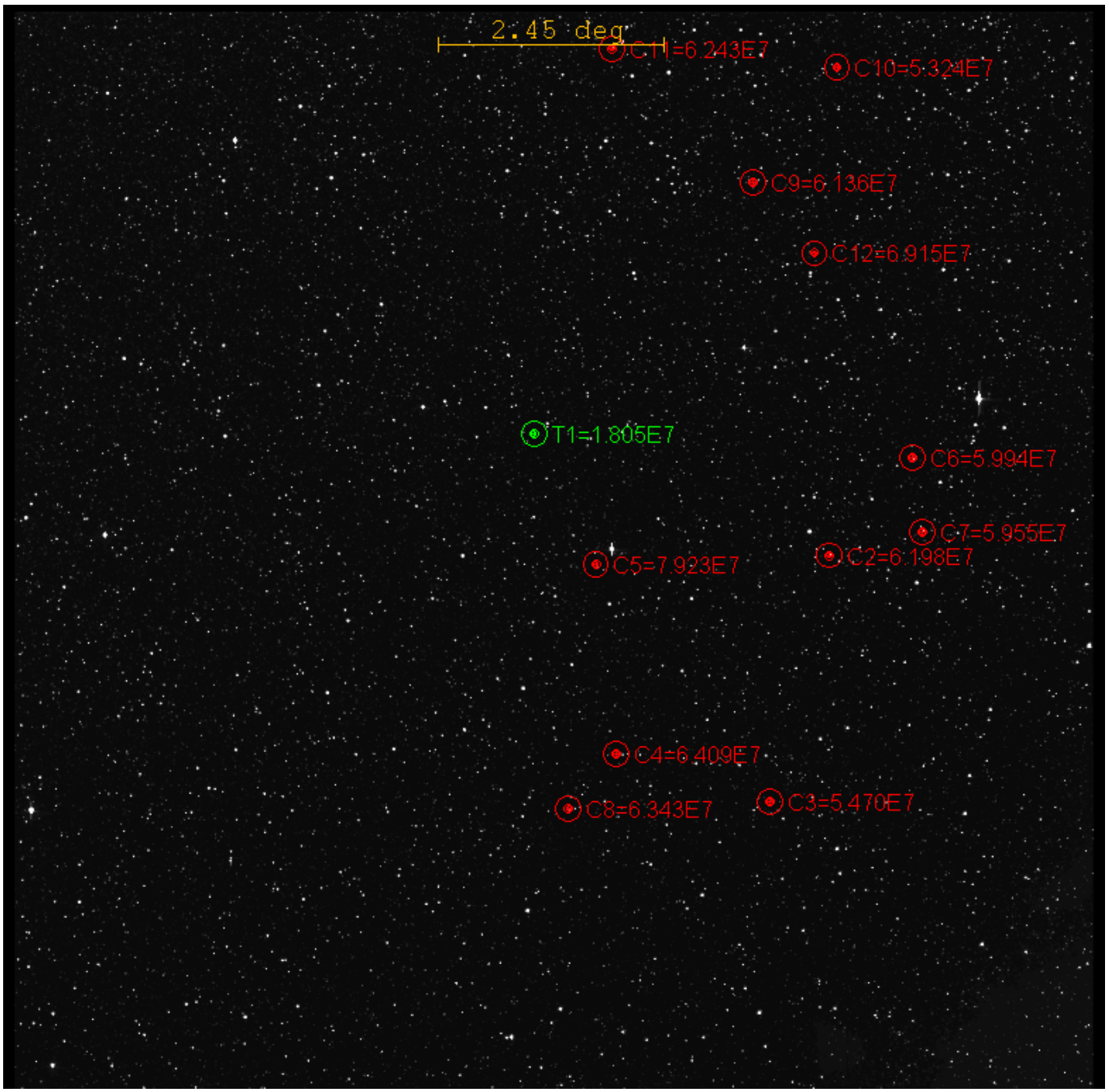

Figure 4: AstroImageJ field view of the KELT-17 target star (T1) and selected comparison stars used for differential photometry of the TESS data set. The space-based observations exhibit a higher signal-to-noise ratio and reduced background variability compared to the ground-based data.

The image displayed below in fig.5 shows the initial photometry light-curve plot for KELT-17 , which includes all comparison stars.

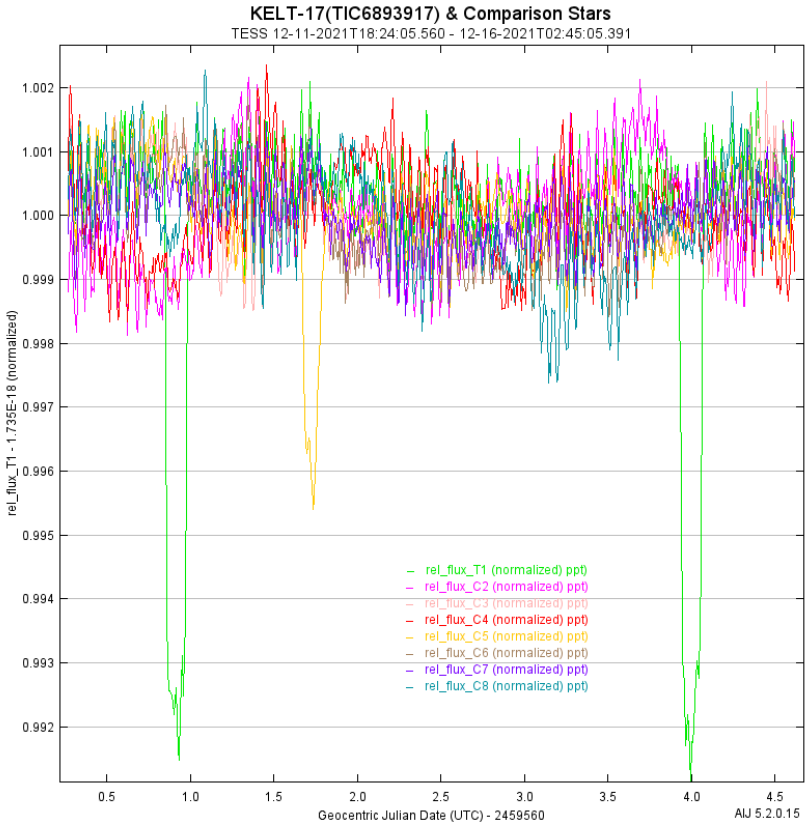

Figure 5: Initial differential photometry light curve for KELT-17 including all selected comparison stars. The increased scatter reflects intrinsic variability in several comparison stars rather than instrumental noise. Two clear transit events of KELT-17b are visible in the target star data.

The plot shown in fig.6 shows target and comparison stars with comparison stars showing high variability removed from the plot to allow cleaner data results from differential calculations. Comparison stars C2, C4 and C8 were removed from the plotted data.

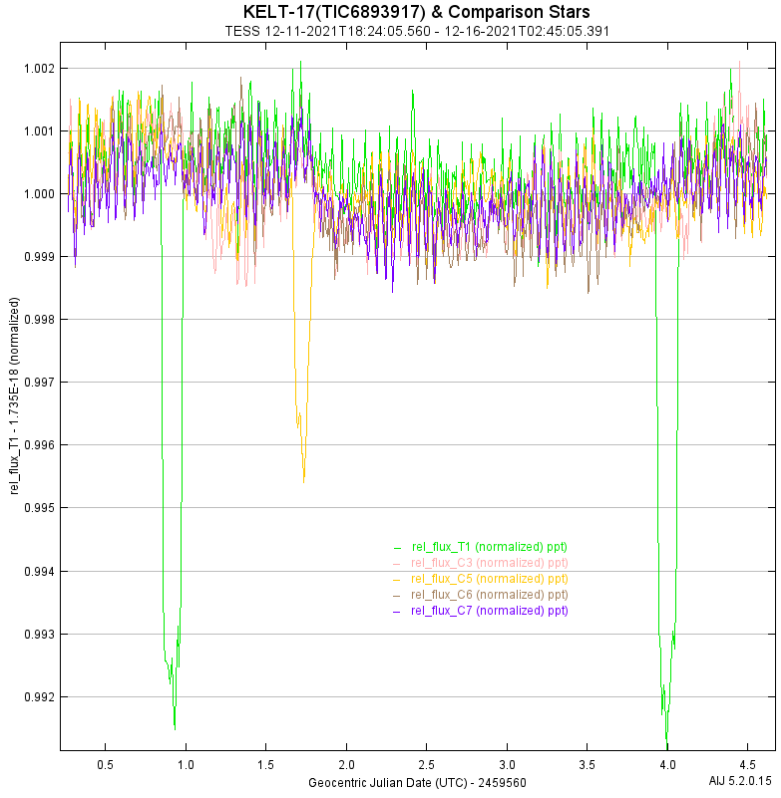

Figure 6: Differential photometry light curve for KELT-17 after removal of highly variable comparison stars (C2, C4, and C8). The remaining comparison stars provide a stable reference, producing a clean detection of two transit events used for subsequent flux-depth and planetary radius calculations.

Plotted output was saved in table format and values for individual data-points used to calculate the 'dip' value (the change in flux). Non-dip averages were determined (for use as a baseline) by using single points on each side of the plotted dips (four in total) in KELT-17's light-curve. Average values for the dips were calculated by taking an average of all values within a dip. (actually done separately and then averaged together). Dip calculations and subsequent planetary radius calculations are shown below.

Average value of points surrounding dip1:
(0.027416808 + 0.027409529) / 2 = 0.0274131685
Average value of points surrounding dip2:
(0.02742249 + 0.027390387) / 2 = 0.0274064385
Combined average value of points surrounding both dips
(0.0274131685 + 0.0274064385) / 2 = 0.0274098035
(A total average value of all non-dip data points yielded a value of 0.02741315 but this report will continue with the combined average value outlined above). This will be used as a baseline to calculate the dip (change in flux) value.

Dip1 average value = 0.027219048 (using excel)
Dip2 average value = 0.027214131 (using excel)
Combined dip average = 0.0272165895

DIP = $1 - dip_{av}/baseline_{av}$ = Δ flux = 0.00704908373

From Eqn1:
$R_p = R_{star}\sqrt{DIP}$ = 1.70169Rsun$\sqrt{0.00704908373}$
= $(1.70169 \times 6.95508 \times 10^8)\ \sqrt{0.00704908373}$
= 99368540.1m = 99368.54051km
= 1.421357734 R_{jup} = 15.5970084 R_{earth}

The known/accepted value chosen from the Exofop - TESS (The California Institute of Technology 2023b) resource provides a planetary radius value of 17.093725 R_{earth}.

The percentage error difference for the results calculated are shown below:

(99368540.1m – 108904122m / 108904122) x 100% = -8.75594213% = -8.8%

4.0 Discussion & Conclusion

4.1 Mount Kent Discussion

The Mt Kent WASP-44 data-set, despite having some issues at the end of the data-set, showed a clear 'dip in the light curve. It was easier to see when offsetting was applied to the plot. The calculations made from values obtained from the differential photometry light-curve plot yielded results that were within 5% of the compared known planetary radius value. The light curve itself didn't appear 'deep' or sharp and this may indicate additional properties of the transit, such as it not being planar to our observation point or non-circular in orbit or a number of other factors that produce light curves of this shape, as indicated by its initial confirmation.(Anderson et al. 2012). The transit of WASP-44b was apparent in the data-set and the calculated values were closer to the known values than initially expected, considering the abbreviated approach taken.

4.2 TESS Discussion

The light curve dips indicating transit, in the case of the KELT-17 data-set, was sharply defined and obvious on the plotted differential photometry light-curve. Only a single comparison star was discarded from final differential evaluation and the variance over time of all stars in the plot appeared low. An additional dip in one of the comparison stars was an interesting surprise and it was left in the final plot as a point of interest.

The calculated planetary radius results were within 10% of the chosen known planetary radius values. Two transits of KELT-17b were apparent in the data-set.

4.3 Ground-based Vs. Space-based Discussion

The TESS KELT-17 data-set required far less preparation prior to photometric analysis than the ground-based data-set. The ground based data analysis also appeared to have more variance in its values due to atmospheric effects. Space-based observatory shows a strong benefit from being able to stay on target far longer.

Conclusion

Both Ground-based and Space-based datasets showed visible transits in their plotted light-curves. The simple calculations made based on the analysis of those data-sets were, both possible, and yielded results more accurate than was anticipated when this investigation began. WASP-44b & KELT-17b showed their presence within the image data investigated. Preparation of the data-sets was likely crucial in allowing a result this definitive. Further refinement of comparison star selection using catalogue-based variability checks could reduce residual scatter in the ground-based light curves in future iterations of this process.

5.0 References

Anderson, D, Collier Cameron, A, Gillon, M, Hellier, C, Jehin, E, Lendl, M, Maxted, P, Queloz, D, Smalley, B & Smith, A 2012, 'WASP-44b, WASP-45b and WASP-46b: three short-period, transiting extrasolar planets', *Monthly Notices of the Royal Astronomical Society*, vol. 422, no. 3, pp. 1988-98.

Collins, KA, Kielkopf, JF, Stassun, KG & Hessman, FV 2017, 'ASTROIMAGEJ: IMAGE PROCESSING AND PHOTOMETRIC EXTRACTION FOR ULTRA-PRECISE ASTRONOMICAL LIGHT CURVES', *The Astronomical Journal*, vol. 153, no. 2, p. 77.

exoplanet kyoto organisation 2023, *Kelt-17*, viewed 09th may 2023, <http://www.exoplanetkyoto.org/exohtml/KELT-17.html>.

Kitchin, CR 2020, *Astrophysical techniques*, CRC press.

Mancini, L, Nikolov, N, Southworth, J, Chen, G, Fortney, JJ, Tregloan-Reed, J, Ciceri, S, van Boekel, R & Henning, T 2013, 'Physical properties of the WASP-44 planetary system from simultaneous multi-colour photometry', *Monthly Notices of the Royal Astronomical Society*, vol. 430, no. 4, pp. 2932-42.

National Aeronautics and Space Administration, N 2022, *TESS Exoplanet Mission*, viewed 27th April, <https://www.nasa.gov/tess-transiting-exoplanet-survey-satellite>.

Saffe, C, Miquelarena, P, Alacoria, J, González, JF, Flores, M, Jaque Arancibia, M, Calvo, D, Jofré, E & Collado, A 2020, 'KELT-17: a chemically peculiar Am star and a hot-Jupiter planet★', *A&A*, vol. 641, p. A145.

Seager, S 2008, 'Exoplanet Transit Spectroscopy and Photometry', *Space Science Reviews*, vol. 135, no. 1, pp. 345-54.

Strasbourg/CNRS, Ud 2023a, *simbad/vizier portal WASP-44*, Harvard-Smithsonian Center for Astrophysics, http://simbad.u-strasbg.fr/simbad/, 10/05/2023, <http://simbad.harvard.edu/simbad/sim-basic?Ident=wasp44&submit=SIMBAD+search>.

Strasbourg/CNRS, Ud 2023b, *simbad portal KELT-17*, Harvard-Smithsonian Center for Astrophysics, http://simbad.u-strasbg.fr/simbad/, 19/04/2023, <http://simbad.cfa.harvard.edu/simbad/sim-id?Ident=TIC6893917>.

The California Institute of Technology, C 2023a, *Exofop: TIC 12862099*, 2023, https://exofop.ipac.caltech.edu/tess/target.php?id=12862099, 12th May 2023, <https://exofop.ipac.caltech.edu/tess/target.php?id=12862099>.

The California Institute of Technology, C 2023b, *Exofop: TIC 6893917*, 2023, https://exofop.ipac.caltech.edu/tess/target.php?id=6893917, 12th May 2023, <https://exofop.ipac.caltech.edu/tess/target.php?id=6893917>.

Wright, D 2023, 'Assessment - Report Information, PHY2204', viewed 22 April 2023,<https://usqstudydesk.usq.edu.au/m2/pluginfile.php/3561119/mod_resource/content/1/PHY2207%20-%20Report%20Information%202022.pdf>.

Zhou, G, Rodriguez, JE, Collins, KA, Beatty, T, Oberst, T, Heintz, TM, Stassun, KG, Latham, DW, Kuhn, RB, Bieryla, A, Lund, MB, Labadie-Bartz, J, Siverd, RJ, Stevens, DJ, Gaudi, BS, Pepper, J, Buchhave, LA, Eastman, J, Colón, K, Cargile, P, James, D, Gregorio, J, Reed, PA, Jensen, ELN, Cohen, DH, McLeod, KK, Tan, TG, Zambelli, R, Bayliss, D, Bento, J, Esquerdo, GA, Berlind, P, Calkins, ML, Blancato, K, Manner, M, Samulski, C, Stockdale, C, Nelson, P, Stephens, D, Curtis, I, Kielkopf, J, Fulton, BJ, DePoy, DL, Marshall, JL, Pogge, R, Gould, A, Trueblood, M & Trueblood, P 2016, 'KELT-17B: A HOT-JUPITER TRANSITING AN A-STAR IN A MISALIGNED ORBIT DETECTED WITH DOPPLER TOMOGRAPHY', *The Astronomical Journal*, vol. 152, no. 5, p. 136.